

11-12  
19367

NASA Technical Memorandum 104376

f 13

# A Model for the Scattering of High-Frequency Electromagnetic Fields from Dielectrics Exhibiting Thermally-Activated Electrical Losses

Raiford E. Hann  
*Lewis Research Center*  
*Cleveland, Ohio*

(NASA-TM-104376) A MODEL FOR THE SCATTERING OF HIGH-FREQUENCY ELECTROMAGNETIC FIELDS FROM DIELECTRICS EXHIBITING THERMALLY-ACTIVATED ELECTRICAL LOSSES  
(NASA) 13 0

NP1-25072  
Unclassified  
CSCL 200 G3/70 0019367

May 1991





A MODEL FOR THE SCATTERING OF HIGH-FREQUENCY ELECTROMAGNETIC  
FIELDS FROM DIELECTRICS EXHIBITING THERMALLY-ACTIVATED  
ELECTRICAL LOSSES

Raiford E. Hann  
National Aeronautics and Space Administration  
Lewis Research Center  
Cleveland, Ohio 44135

SUMMARY

An equivalent circuit model (ECM) approach is used to predict the scattering behavior of temperature-activated, electrically lossy dielectric layers. The total electrical response of the dielectric (relaxation + conductive) is given by the ECM and used in combination with transmission line theory to compute reflectance spectra for a Dallenbach layer configuration. The effects of thermally-activated relaxation processes on the scattering properties is discussed. Also, the effect of relaxation and conduction activation energy on the electrical properties of the dielectrical properties of the dielectric is described.

INTRODUCTION

Scattering of high-frequency electromagnetic fields from dielectric surfaces is a phenomenon of interest in the design of many microwave and millimeter wave systems. A wealth of information on reflection analysis and absorber design is available in the literature dating back to the 1950's; however, very little information on the relationship of the temperature dependent properties of dielectrics on their high-frequency scattering behavior currently exists. In this paper, a model for the thermally activated scattering response of a dielectric Dallenbach layer configuration is given. The model is based on the thermally-activated, total electrical response of a conductive dielectric as represented by an equivalent electrical circuit containing both discrete and distributed elements.

DIELECTRIC RELAXATION THEORY

In order to predict the scattering of electromagnetic fields from dielectrics, the electrical response of the bulk dielectric to a time-varying field must first be defined. This involves an analysis of both the system's dielectric and conductive properties.

The complex permittivity of a dielectric containing mobile charge carriers is given by the relationship,

$$\epsilon^* = [(\epsilon_s - \epsilon_\infty)/(1 + (i\omega T)^{1-\alpha}) + \epsilon_\infty] - i\sigma_{DC}/\omega. \quad (1)$$

The first term is the dielectric function given by Cole and Cole (ref. 1) where  $\epsilon_s$  and  $\epsilon_\infty$  are the static and high-frequency limiting permittivities,  $T$  is the mean dielectric relaxation time,  $i$  is equal to  $\sqrt{-1}$  and indicates an imaginary quantity,  $\omega$  is the angular frequency and  $\alpha$  is a parameter describing the shape of the relaxation spectra. For the limiting case of  $\alpha = 0$ , the Cole-Cole function simply

reduces to the Debye model. The second term represents the loss resulting from the dc conductivity of the dielectric. The dc conductivity results from the long-range migration of the charge-carrying species and is frequency independent. Figure 1 shows a comparison of loss spectra for a Debye model dielectric with two spectra generated with the Cole-Cole function for different values of  $\alpha$ . It can be seen that as the value of  $\alpha$  increases, the width of the spectral profile broadens. This broadening effect has been interpreted as a result of a distribution of relaxation times (refs. 2 and 3) associated with charge carrier-vacancy re-orientation and is typically observed in real conductive dielectric systems (refs. 4 and 5).

Both  $\tau$  and  $\sigma_{DC}$  typically exhibit Arrhenius type thermally activated behavior (ref. 6), which may be expressed as,

$$\sigma_{DC} = \sigma_0 e^{-E/k_B T} \quad (2)$$

and,

$$\tau = \tau_0 e^{E/k_B T}. \quad (3)$$

Here,  $\sigma_0$  and  $\tau_0$  are pre-exponential factors,  $E$  is the activation energy for charge carrier migration and relaxation,  $k_B$  is the Boltzman constant, and  $T$  is the absolute temperature. We will assume that the activation energies are equal for the conduction and relaxation processes and the validity of this assumption will be discussed in the next section.

The total dielectric response of the conductive dielectric system may be modeled using the equivalent circuit shown in figure 2. The complex admittance of this circuit is given by,

$$Y^*(\omega, T) = 1/R(T) + i\omega C_\infty + 1/[1/(i\omega \Delta C) + Z_{CPE}(\omega, T)] \quad (4)$$

where  $C_\infty = \epsilon_\infty \epsilon_0$ ,  $\Delta C = (\epsilon_s - \epsilon_\infty) \epsilon_0$ ,  $R(T) = 1/\sigma_{DC}$  and  $\epsilon_0$  is the permittivity of free space.  $Z_{CPE}$  is a special function known as the "constant phase element" (CPE) whose name is derived from the fact that the phase angle of its response has a characteristic constant value of  $a\pi/2$ . The CPE is a useful mathematical device for simulating non-Debye relaxation processes which are believed to result from relaxation time distributions previously mentioned (ref. 7). In terms of the equivalent circuit model (ECM), the CPE is a distributed circuit element and may be described as a frequency-dependant capacitor. The expression for the CPE is,

$$Z_{CPE} = A(i\omega)^{-\alpha} \quad (5a)$$

where

$$A = \tau_0^{1-\alpha}/[(\epsilon_s - \epsilon_\infty) \epsilon_0]. \quad (5b)$$

The ECM provides a practical method for modeling the bulk response of dispersive dielectrics and their thermally-activated behavior. Assuming no crystallographic or microstructural changes occur for a given material, the electrical response may be predicted quite accurately for a wide temperature range over several decades in frequency. Based on this property, the bulk response model may be used in combination with transmission line theory to predict the scattering behavior of layer configurations.

## SCATTERING THEORY

Using the ECM, normal incidence scattering from a Dallenbach design (ref. 8) dielectric system will be considered. The configuration consists of an electrically homogeneous, lossy dielectric layer backed by a highly conductive surface. This design is used commonly with thin layer systems to facilitate absorption of microwave fields by resonant cancellation (ref. 8).

In order for resonant cancellation of an electromagnetic field to occur in a Dallenbach system, a phase shift must occur as the transmitted component of the field traverses the thickness of the layer, reflects off of the conductive ground plane, and reemerges at the surface of the layer. Electrical losses,  $\epsilon'$  and the physical thickness of the bulk dielectric are responsible for the phase shift which, under the proper conditions, allow the reemergent field components to destructively interfere with components reflected solely at the front surface of the dielectric. The result of this phenomenon is a minimum in the total reflected energy from the surface for a layer having an electrical thickness, defined as  $d_e = [\epsilon' \mu']^{1/4} x$  (physical thickness), equal to an odd multiple of a quarter-wavelength with respect to the incident field.

Scattering from a Dallenbach design may be predicted by transmission line theory (ref. 8). This analysis is accomplished by defining the bulk complex constitutive properties of the layer,  $\epsilon$  and  $\mu$ , and the thickness of the layer. The intrinsic impedance of the layer is given by,

$$Z = [\mu/\epsilon]^{1/4} \quad (6)$$

where  $\mu$  is the complex permeability of the layer. The complex wavenumber,  $k$ , is given by,

$$k = w/c[\epsilon\mu]^{1/4}. \quad (7)$$

Using these quantities the effective input impedance,  $\beta$ , may be determined by,

$$\beta = iz \tan(kd) \quad (8)$$

where  $d$  is the physical thickness of the layer. The voltage reflection coefficient may be computed by the relationship,

$$\Gamma = (\beta - 1)/(\beta + 1). \quad (9)$$

Obviously,  $\Gamma$  is a complex quantity containing both amplitude and phase information; however, the magnitude,  $|\Gamma|$ , will be sufficient for this model.

At this point, the mathematical aspects of the model have been fully described. In the next section, reflectance spectra generated by the model will be presented and examined in terms of calculated, thermally-activated properties of a hypothetical dielectric layer.

## MODELING RESULTS

In order to present a generalized description of the temperature-activated electrical response and to limit the large number of possible results, a number of simplifying constraints and assumptions associated with the ECM have been made. It

should be noted that although the assumptions are used in the case presented here, there is no reason why they must be applied to other cases.

It is assumed in this model that the thermally-activated dielectric and conductive properties are controlled exclusively by the quantity,  $E/k_B T$ . In order to generalize the model, the normalized energy function,  $\theta$ , will be defined as  $\theta = E/k_B T$ . Also, the constraint  $E_{\text{RELAXATION}} = E_{\text{DC}}$  will be applied. The validity of this action is based on a large body of experimental data and has been reviewed by Tomazawa (ref. 9). Since different combinations of  $E$  and  $k_B T$  will yield the same value of  $\theta$ , and hence identical reflectance spectra, the thermally activated effects will first be described in terms of  $\theta$  in order to avoid this ambiguity. Later in this section, a set of reflectance spectra will be presented for various values of  $E$  at different temperatures. Although less general in nature, these curves may provide a more practical assessment of the predictions. Lastly, it is assumed that the layer is nonmagnetic; therefore,  $\mu = 1$ .

Table I contains the parameters used to calculate the reflection spectra presented in this section. The values selected for these parameters were chosen from ranges consistent with real dispersive oxide conductors. Since a wide variety of responses may be computed based on the various combinations of parameters, only one case will be presented which will illustrate typical thermally activated behavior.

In order to fully understand the calculated reflectance spectra we must first examine the predicted temperature-dependent bulk properties based on the ECM presented earlier. Variations in the real component of the permittivity with  $\theta$  are illustrated in figure 3. It can be seen that as  $\theta$  decreases an increase in  $\epsilon'$  is predicted over the frequency space where relaxation occurs. In the high and low frequency regions,  $\epsilon'$  approaches the  $\epsilon_\infty$  and  $\epsilon_s$  limiting values. It should be noted that frequency superposition may be applied to these spectra where one curve can be perfectly superimposed on another by a translation in frequency space. The amount of frequency translation necessary depends on the difference in the respective  $\theta$  values.

Figures 4(a), (b), and (c) show the loss spectra for  $\theta$  values of 9.5, 7.5, and 5.5, respectively. A full logarithmic scale was used in order to give a better comparison for the different values of  $\theta$ . At the lower frequency values, loss due to the dc conduction process is observed to be the predominant loss mechanism. As the frequency increases a cross-over point occurs where relaxation losses become more dominant; however, the total loss of the system rapidly diminishes. This effect is seen to be most pronounced for the dc component. As  $\theta$  decreases, the cross-over point moves higher in frequency resulting primarily from an increase in  $\sigma_{\text{DC}}$ . In the logarithmic representation of the loss spectra, a linear relationship holds for  $\sigma_{\text{DC}}$  with frequency and is given by,

$$\log(\sigma_{\text{DC}}'') = \log(\sigma_{\text{DC}}) - \log(W). \quad (10)$$

Therefore, the increase in the dc component of the loss is exclusively due to an increase in  $\sigma_{\text{DC}}$ . It should be noted that for  $\theta \leq 6$ , the lower frequency losses become extremely high and are composed primarily of the dc component.

The semi-logarithmic representation of the relaxation loss spectra shown in figure 5(a) reveal the shift in the position of the loss maxima in frequency space for different values of  $\theta$ . The relationship of the positions of the loss maxima with the energy function,  $\theta$ , is illustrated in figure 5(b). Here, the Arrhenius

behavior of the relaxation process, given by equation (3), is observed. An important point to note is that unlike the dc conduction losses, the integrated loss due to relaxation remains constant, regardless of the value of  $\theta$ . The magnitude of the relaxation loss generally depends on the relaxation strength,  $(\epsilon_s - \epsilon_\infty)$  and to a lesser extent on  $a$ .

We now turn to examine the reflection spectra which were calculated based on the bulk properties predicted by the ECM. In figure 6, reflection spectra calculated for five values of  $\theta$  are shown. On inspection, two trends are observed. For the first trend, we see that as  $\theta$  decreases from the value of 9.5 to 8.5, the reflection minimum becomes deeper. This indicates that a more optimum interference condition is occurring for this particular combination of layer thickness and electrical loss. As  $\theta$  decreases below 8.5 the interference condition begins to move away from optimum.

The second effect observed is the shift in the reflection minima to lower frequencies with decreasing  $\theta$ . This effect is a result of an increase in the electrical thickness, which, in turn is due to an increase in  $\epsilon'$ . This increase in  $\epsilon'$  was discussed earlier in relation to figure 3. As expected, the reflectance increases significantly as  $\theta$  continues to decrease, which results directly from the rapidly increasing dc conduction losses as illustrated in figure 4.

In the next set of reflectance spectra, the effects of activation energy and temperature have been separated. These spectra are presented in the context that the different activation energies represent different layer materials. Although a simplifying assumption has been made that the remaining parameters are the same for the different hypothetical materials, this should not seriously endanger the validity of the illustration.

The effect of temperature on the scattering behavior of layers having three different activation energies are shown in figure 7. For layer A (fig. 7(a)), we see an approach to the optimum interference condition with increasing temperature, which is expected to be achieved for a temperature slightly higher than 1200 °C. For layer B (fig. 7(b)), the optimum condition occurs at a much lower temperature due to the lower value of  $E$  for the material. In contrast to layer A, it can be seen that the temperature at which the optimum interference condition occurs for layer C (fig. 7(c)) falls well below the temperature range selected for this calculation. These results simply illustrate that the electrical losses required for resonant cancellation are achieved at lower temperatures for materials with lower conduction activation energies. It should also be noted that the shift of the reflection minima to lower frequencies becomes more pronounced for lower activation energies. This effect would be more apparent for cases where the activation energies for relaxation and dc conduction were independent. As discussed previously, the shift is directly related to an increase in  $\epsilon'$  with decreasing values of the energy function.

## CONCLUSIONS

A model which illustrates the effect of thermally-activated losses on the scattering behavior of dielectric layers has been presented. The model provides a method for predicting how various temperature-dependent dielectric and conductive properties affect the reflection of high-frequency fields from layer geometries. Applications to be considered for the model may include dielectric absorber and resonator design for high-temperature environments.

The crux of this discussion has primarily consisted of two points; (1) the thermal dependence of  $\epsilon'$  and its resulting effect on the position of the reflection minima and (2) the effect of the total electrical loss on the interference condition. Also, in terms of the energy function, the losses required for resonant cancellation occur at much lower temperatures for lower activation energy materials.

It should be noted that there are other classes of non-Debye model dielectrics whose responses deviate somewhat from single, dispersive, "CPE" type behavior presented here. In some cases, the electrical response may be represented by an equivalent circuit consisting of two parallel CPE's, known as the Joncher response (ref. 10). Other more sophisticated models which have been used to analyze the response of conductive dielectrics containing two power-law regions include the fractal cluster model established by Dissado and Hill (ref. 12). The scattering behavior for dielectrics based on these models may be considerably different than that of the single CPE model. Currently, work is in progress in this laboratory on expanding the model presented in this paper to include other dielectric response formalisms.

#### REFERENCES

1. K.S. Cole and R.H. Cole, "Dispersion and Absorption in Dielectrics," *J. Chem. Phys.*, vol. 9, pp. 341-351, Apr. 1941.
2. V.V. Daniel, Dielectric Relaxation, New York: Academic Press, 1967, pp. 95-109.
3. J.R. MacDonald, "Linear Relaxation: Distributions, Thermal Activation, Structure, and Ambiguity," *J. Appl. Phys.*, vol. 62, no. 11, pp. R51-R62, 1987.
4. H.E. Taylor, "An Investigation of the Dielectric Relaxation Exhibited by Glass: Part II," *J. Soc. Glass Tech.*, vol. 43, no. 211, pp. 124-146, 1959.
5. D.P. Almond and A.R. West "Impedance and Modulus Spectroscopy of 'Real' Dispersive Conductors," *Solid State Ionics*, vol. 11, pp. 57-64, 1983.
6. W.D. Kingery, H.K. Bowen, and D.R. Uhlmann, Introduction to Ceramics, 2nd ed., New York: John Wiley and Sons, 1976, pp. 875, 938.
7. J.R. MacDonald, "Some Simple Equivalent Circuits for Ionic Conductors," *J. Electroanalytical Chem.*, vol. 200, pp. 69-82, 1986.
8. E.F. Knott, J.F. Schaeffer, and M.T. Tuley, Radar Cross Section, Norwood, MA: Artech House, 1985, pp. 47-50.
9. M. Tomozawa, Dielectric Characteristics of Glass. Glass I: Interaction with Electromagnetic Radiation, Treaties on Materials Science and Technology, vol. 12, M. Tomozawa and R.M. Doremus, eds., London: Academic, 1977, pp. 283-345.
10. L.A. Dissado and R.M. Hill, "The Fractal Nature of the Cluster Model Response Functions," *J. Appl. Phys.*, vol. 66, no. 6, pp. 2511-2524, 1989.

TABLE I.  
 [The following parameter values were used to generate the reflectance spectra.]

$\epsilon_s$	= 50
$\epsilon'$	= 6
$\alpha$	= 0.333
$d$	= 0.154 cm
$\theta$	= 9.5, 8.5, 7.5, 6.5, 5.5

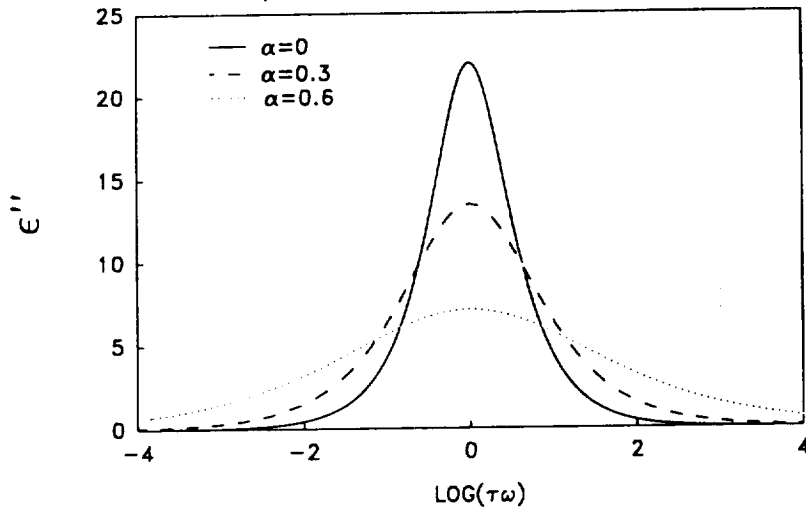


Figure 1.—Comparison of the loss spectra of a Debye model dielectric with the Cole-Cole model for different values of  $\alpha$ .

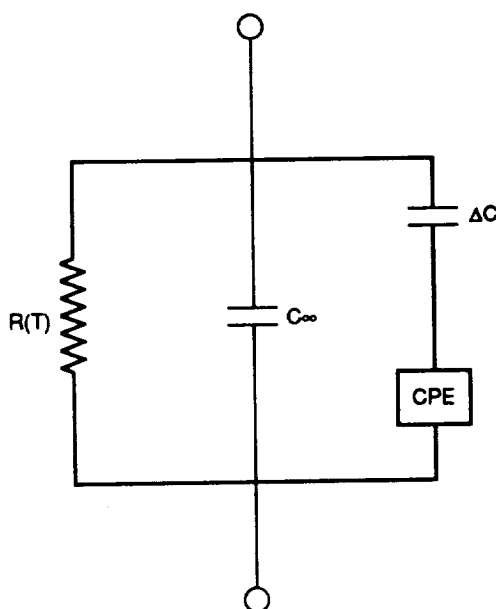


Figure 2.—Equivalent circuit with "constant phase element" for a conductive dielectric.

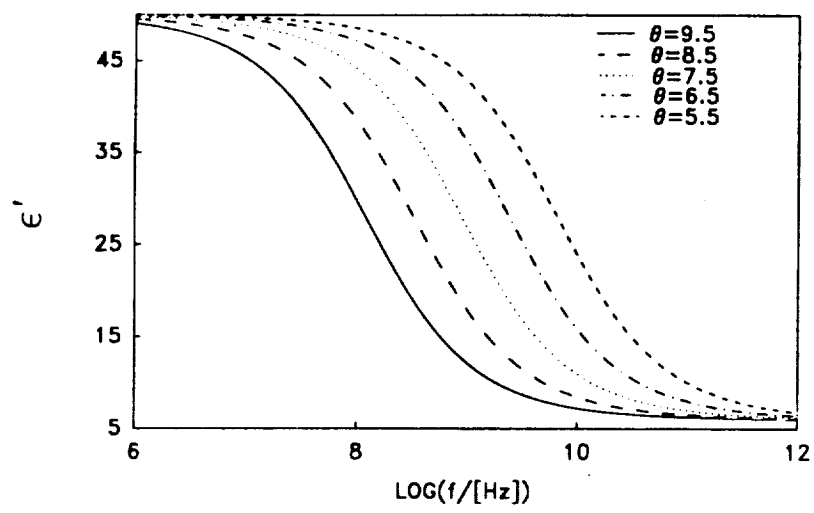


Figure 3.—Calculated permittivity spectra showing frequency and energy dependence of  $\epsilon$ .

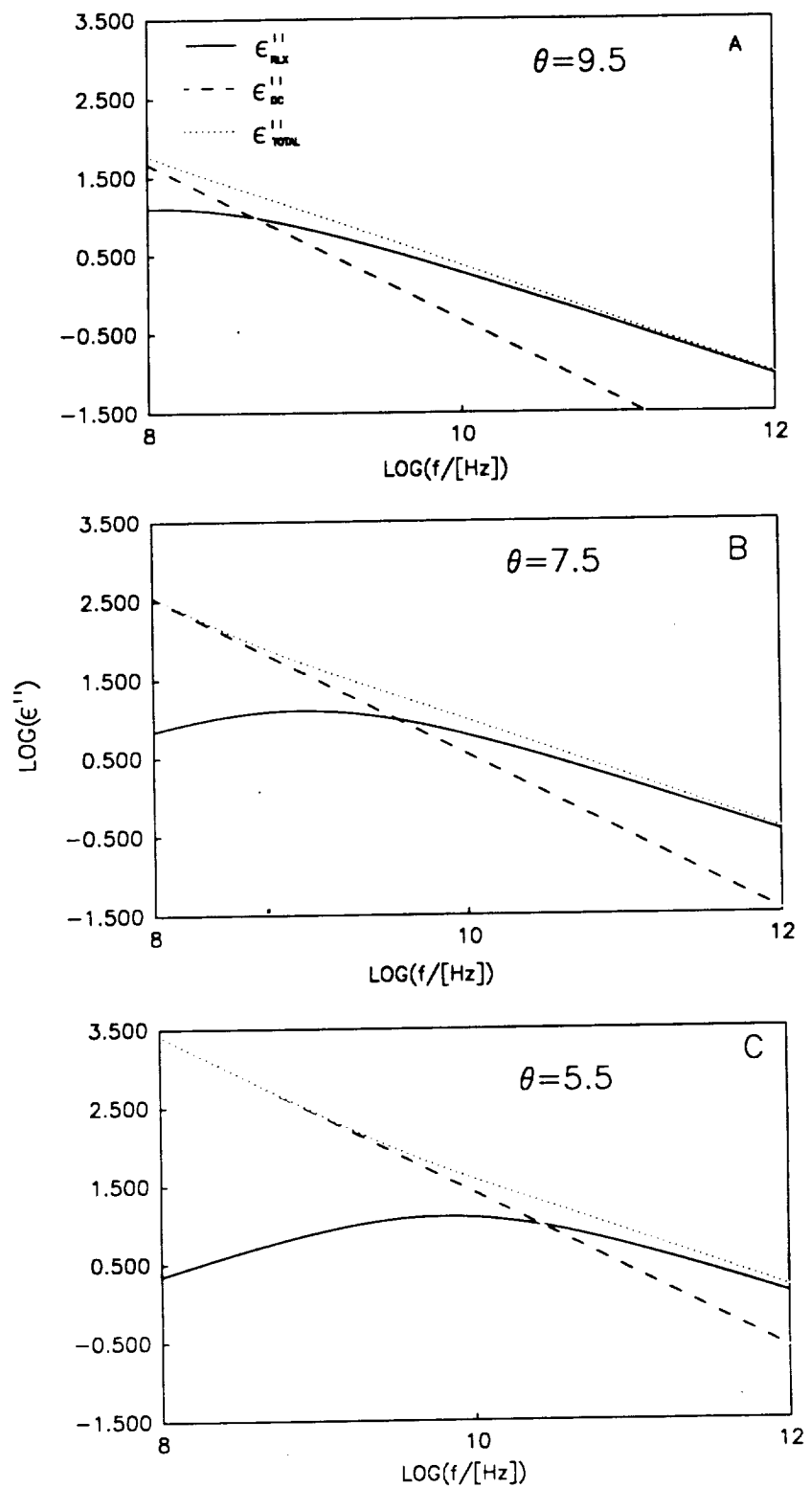


Figure 4.—Loss spectra calculated for  $\theta$  values of (a) 9.5, (b) 7.5 and (c) 5.5.

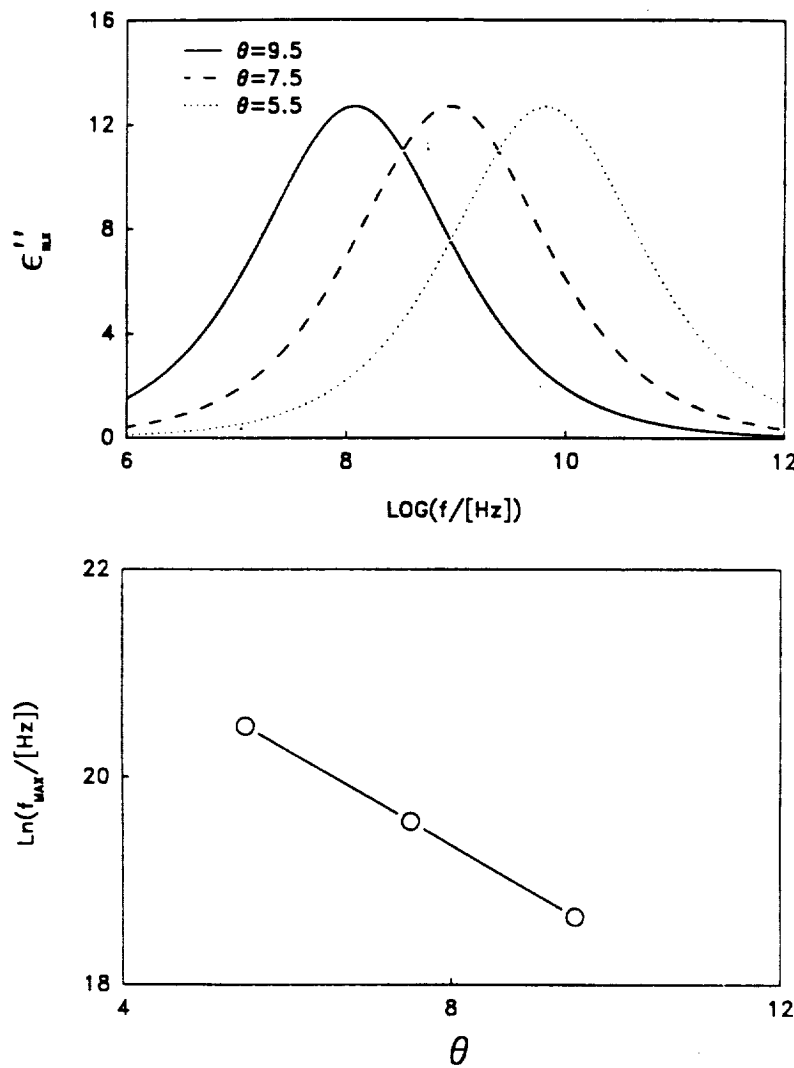


Figure 5.—Calculated relaxation loss spectra showing dependence of the position of peak maxima (a) and Arrhenius plot showing the calculated thermal activation of the relaxation loss peak maxima (b).

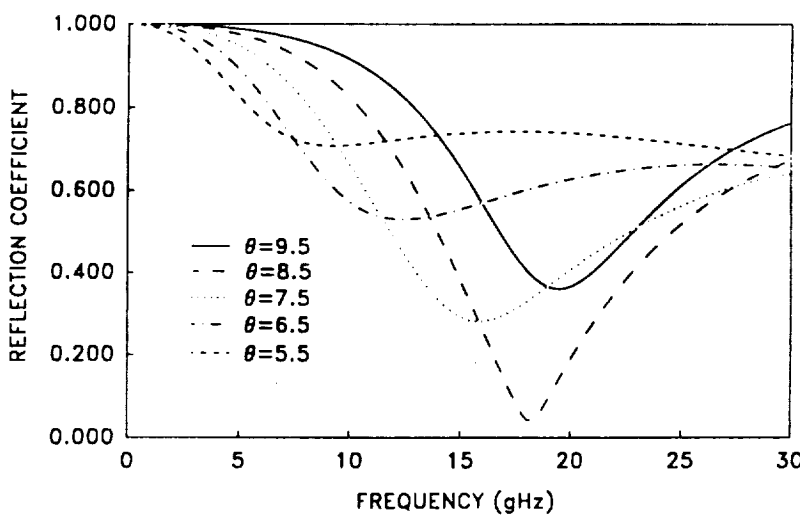


Figure 6.—Reflectance spectra calculated for various values of  $\theta$ .

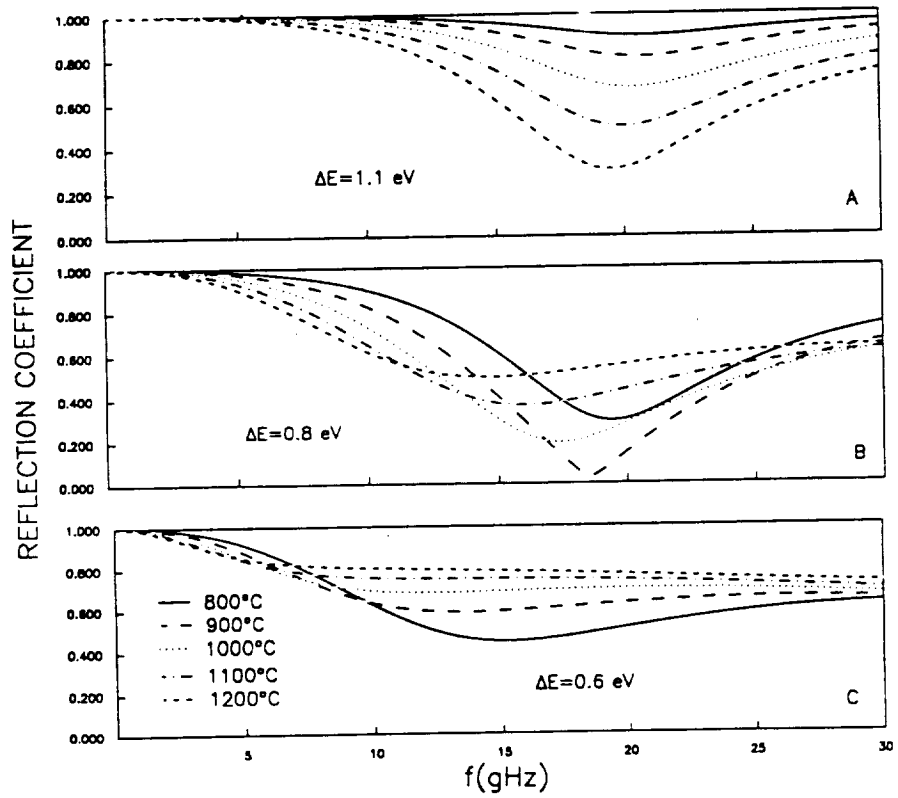


Figure 7.—Reflectance spectra calculated for various temperatures with  
 $\Delta E$  = (a) 1.1 eV (b) 0.8 (c) 0.6 eV.



National Aeronautics and  
Space Administration

## Report Documentation Page

1. Report No. <b>NASA TM -104376</b>	2. Government Accession No.	3. Recipient's Catalog No.	
4. Title and Subtitle <b>A Model for the Scattering of High-Frequency Electromagnetic Fields from Dielectrics Exhibiting Thermally-Activated Electrical Losses</b>		5. Report Date <b>May 1991</b>	
		6. Performing Organization Code	
7. Author(s) <b>Raiford E. Hann</b>		8. Performing Organization Report No. <b>E -6040 -1</b>	
		10. Work Unit No. <b>505 -62</b>	
9. Performing Organization Name and Address <b>National Aeronautics and Space Administration Lewis Research Center Cleveland, Ohio 44135 - 3191</b>		11. Contract or Grant No.	
		13. Type of Report and Period Covered <b>Technical Memorandum</b>	
12. Sponsoring Agency Name and Address <b>National Aeronautics and Space Administration Washington, D.C. 20546 - 0001</b>		14. Sponsoring Agency Code	
15. Supplementary Notes Responsible person, Raiford E. Hann, (216) 433 - 8008.			
16. Abstract An equivalent circuit model (ECM) approach is used to predict the scattering behavior of temperature-activated, electrically lossy dielectric layers. The total electrical response of the dielectric (relaxation + conductive) is given by the ECM and used in combination with transmission line theory to compute reflectance spectra for a Dallenbach layer configuration. The effects of thermally-activated relaxation processes on the scattering properties is discussed. Also, the effect of relaxation and conduction activation energy on the electrical properties of the dielectric is described.			
17. Key Words (Suggested by Author(s)) <b>Electromagnetic fields Reflectance Temperature dependence</b>		18. Distribution Statement <b>Unclassified - Unlimited Subject Category 70</b>	
19. Security Classif. (of the report) <b>Unclassified</b>	20. Security Classif. (of this page) <b>Unclassified</b>	21. No. of pages <b>12</b>	22. Price* <b>A03</b>



National Aeronautics and  
Space Administration

**Lewis Research Center**  
Cleveland, Ohio 44135

FOURTH CLASS MAIL

ADDRESS CORRECTION REQUESTED

Official Business  
Penalty for Private Use \$300



Postage and Fees Paid  
National Aeronautics and  
Space Administration  
NASA 451

**NASA**

---